scientific reports

Check for updates

OPEN

Initial evidence of abnormal brain plasticity in anorexia nervosa: an ultra-high field study

Edoardo Pappaianni[1], Bianca Borsarini[1], Gaelle E. Doucet[2], Ayelet Hochman[3], Sophia Frangou[4,5] & Nadia Micali[1,6,7]✉

Anorexia Nervosa has been associated with white matter abnormalities implicating subcortical abnormal myelination. Extending these findings to intracortical myelin has been challenging but ultra-high field neuroimaging offers new methodological opportunities. To test the integrity of intracortical myelin in AN we used 7 T neuroimaging to acquire T1-weighted images optimized for intracortical myelin from seven females with AN (age range: 18–33) and 11 healthy females (age range: 23–32). Intracortical T_1 values (inverse index of myelin concentration) were extracted from 148 cortical regions at ten depth-levels across the cortical ribbon. Across all cortical regions, these levels were averaged to generate estimates of total intracortical myelin concentration and were clustered using principal component analyses into two clusters; the outer cluster comprised T_1 values across depth-levels ranging from the CSF boundary to the middle of the cortical regions and the inner cluster comprised T_1 values across depth-levels ranging from the middle of the cortical regions to the gray/white matter boundary. Individuals with AN exhibited higher T_1 values (i.e., decreased intracortical myelin concentration) in all three metrics. It remains to be established if these abnormalities result from undernutrition or specific lipid nutritional imbalances, or are trait markers; and whether they may contribute to neurobiological deficits seen in AN.

In the central nervous system, myelin is a cholesterol rich extension of oligodendrocytes that coats axons, i.e. the long processes of neurons[1,2]. Axon myelination in the nervous system enables fast, saltatory electrical impulse propagation through action potentials modulation. Myelin can be thought of as an insulator, which boosts the conduction speed of the action potential along the axonal body, increasing the neural signal transmissibility from neuron to neuron, ultimately sustaining adequate cerebral intra-and-inter regional communication[2]. Motor, sensory, and cognitive functions of the nervous system all require rapid impulse propagation relying on an adequate axonal myelination[2,3]. Not only does myelin surround white matter bundles, it also plays a key role in cortical gray matter. Intracortical myelin is most prevalent in the deeper layers of the cortex, and it seems to enhance cortical function by fine-tuning timing and synchrony of neural networks[4]. Being particularly sensitive to experience[3] and in continuous development throughout life[5], intracortical myelin participates in brain plasticity and remodeling. This is evidenced by the fact that myelin content is associated with cognitive function, and that higher levels of intracortical myelin are associated with better performance on cognitive tasks[5]. Therefore, it is safe to assume that an abnormal concentration of intracortical myelin may play a role in psychiatric disorders. This is the case with schizophrenia, where a loss of intracortical myelin has been shown[3,6,7].

Animal studies have provided consistent support for an adverse impact of undernutrition on myelination, given the potentially detrimental effects of long-lasting starvation on white matter (WM) composition[8,9]. Despite the lack of equivalent investigations in humans, myelin seems to be sensitive to micro-and-macro nutrient deficiencies: in fact, evidence in the literature suggests that iron is directly involved in myelin production as a required co-factor for cholesterol and lipid biosynthesis[10]. Authors have suggested that inflammation, oxidative stress, and loss of oligodendrocytes might all play a role[11–13].

Anorexia nervosa (AN) is a severe psychiatric disorder with one of the highest long-term mortality rates of all psychiatric disorders[14–16]. It affects predominantly women, emerging typically during adolescence and early

[1]Department of Psychiatry, Faculty of Medicine, University of Geneva, 2 Rue Verte, 1205 Geneva, Switzerland. [2]Boys Town National Research Hospital, Omaha, NE, USA. [3]Department of Psychology, St. John's University, Queens, NY, USA. [4]Department of Psychiatry, Icahn School of Medicine at Mount Sinai, New York, NY, USA. [5]Department of Psychiatry, University of British Columbia, Vancouver, BC, Canada. [6]Great Ormond Street Institute of Child Health, University College London, London, UK. [7]Department of Pediatrics, Gynecology and Obstetrics, Faculty of Medicine, University of Geneva, Geneva, Switzerland. ✉email: nadia.micali@hcuge.ch

	AN patients	Controls	Group differences
Age (years)	25.14 (5.21)	27.18 (3.28)	ns^{+}
BMI (kg/m^2)	17.34 (0.63)	23.03 (3.02)	t = 6.057, p < 0.001
Osmolality (mmol/kg)*	289.71 (16.53)		
EDE: global score	2.54 (0.93)		
EDE: restraint	2.49 (1.34)		
EDE: eating concern	1.89 (1.42)		
EDE: shape concern	3.20 (0.99)		
EDE: weight concern	2.57 (1.03)		

Table 1. Descriptive statistics: *Osmolality index expressed in milliosmoles/kg. Mean (standard deviation) and group differences for age and BMI are shown. Average osmolality index, EDE's global score, restraint, eating concern, shape concern and weight concern subscales score are reported for individuals with AN only. EDE, Eating Disorder Examination. $^{+}p > 0.05$.

adulthood[17]. The core features of the disease are an intense fear of gaining weight, a body-image distortion leading to weight loss, behaviors and strategies aimed at weight loss and resulting in a state of severe malnutrition[18]. There is growing evidence of the impact of AN on the brain, both on structure and function[19–25]. In particular, WM microstructure alterations, gray and WM volume abnormalities have been shown in patients with AN in both acute and chronic phases[20–22,26–29].

Given that animal models suggest a myelin decrease following malnutrition, the evidence of intracortical myelin abnormalities in other psychiatric disorders, and its maturational pattern (that extends into late adolescence and adulthood)[30–32], it is reasonable to hypothesize a myelin deficit in patients with AN. However, since in AN WM investigations have been almost-exclusively carried out with standard Magnetic Resonance Imaging (MRI) acquisition sequences, a direct quantitative detection of myelin concentration in-vivo has been challenging[33].

New techniques based on ultra-high field MRI imaging[34–38] may address this gap in the literature, allowing visualization of the brain at submillimeter resolution[39] and examination of myelin in a more fine-grained fashion. In view of the fact that the human cortex is approximately 2–4 mm thick, standard spatial resolution (1 mm) does not allow for proper detection of intracortical myelin[40]. Moreover, evidence shows that depth-dependent intracortical myelin properties obtained by ultra-high field MRI are reliable and consistent with ex-vivo data[34,39,40]. Based on this premise, in our preliminary study we aimed to measure intracortical myelin in patients with AN and controls, capitalizing on a newly validated method able to ascertain depth-dependent intracortical myelin organization with an ultra-high field 7 T scanner[39,40]. Specifically, using an ad-hoc acquisition sequence and data analysis procedure, in-vivo T_1 values (in milliseconds) as inverse measure of intracortical myelin[39] were extracted and compared in a sample of women with AN and healthy controls. To our knowledge, this type of investigation of cortical myelo-architecture has never been carried out in AN. Moreover, the use of quantitative MRI to measure actual tissue parameters (such as T_1 values) prevents the risk of tissue or hardware-related bias that may impact generalizability of results[41]. We hypothesized that individuals with AN would show higher T_1 values (i.e., lower intracortical myelin concentration) compared to controls. We also explored whether the differences in intracortical myelin concentration would be particularly visible in the outermost cortical vs. innermost depth-levels in AN. We further investigated any relationships between disorder-related variables and intracortical myelin.

Results

Socio-demographic and illness-related data. Individuals with AN did not differ from controls in terms of age. As expected, individuals with AN had a significantly lower Body Mass Index (BMI) compared to controls (Welch $t = 6.057$, $p < 0.001$) (Table 1). Osmolality levels were within the normal range for 4/7 (57.1%) individuals with AN, while three patients had slightly higher values than the normal range[42]. Duration of illness in individuals with AN ranged between 1 and 21 years. No current psychiatric comorbidity, or past psychiatric diagnosis was identified. Only one participant reported psychotropic medication use (venlafaxine).

Global T1 values. Participants with AN and controls had equal variances distribution for total T_1 values (in milliseconds) (Levene's Test $p > 0.05$). A statistically significant difference emerged between groups for T_1 values ($F(1,15) = 6.95$, $p = 0.03$, $\eta^2 = 0.29$). In detail, patients with AN showed higher T_1 values than controls (Mean Difference MD = 48.55 ms, Standard Error SE = 19.80, 95% Confidence Intervals (C.I.) = 6.34, 90.77, Cohen's $d = 1.26$). These differences also emerged in the bootstrap post-hoc comparison (MD = 48.28 ms, Bias = −0.406, SE = 17.29, 95% bias corrected accelerated C.I. = 15.28, 85.14). See Table 2 and Fig. 1b for all details. A graphical representation of total T_1 values maps is available in Fig. 1a. Images were rendered with the *ggsegDesterieux* (https://github.com/LCBC-UiO/ggsegDesterieux) and *ggseg*[43] (https://lcbc-uio.github.io/ggseg/) packages via RStudio v. 1.2.50. working on R v.4.0.4.

Based on the structural indications provided by the Principal Component Analysis (PCA), we averaged the T_1 values from depth levels 1 to 5 independent of ROIs to form a composite measure of intracortical concentration in an "inner cluster" (i.e., cluster extending from the middle of the cortical ribbon to the gray matter/white matter boundary). The corresponding measures from depth levels 6 to 10 were also averaged independent of ROIs to generate a composite measure of intracortical concentration in an "outer cluster" (i.e., cluster extending

	AN	Controls	Group differences[a]
T_1 values (ms)—total intracortical myelin concentration	1858.96 (28.08)	1809.95 (43.47)	$F(1,15) = 6.01$, $p = 0.03$, $\eta^2 = 0.29$

Table 2. Global T_1 values across individuals with AN and controls: Analysis of Covariance. Mean (standard deviation) of average T_1 values across all ten cortical depth-levels. Group differences in terms of F value (degrees of freedom), p value and effect size are shown. [a]Analysis corrected for age.

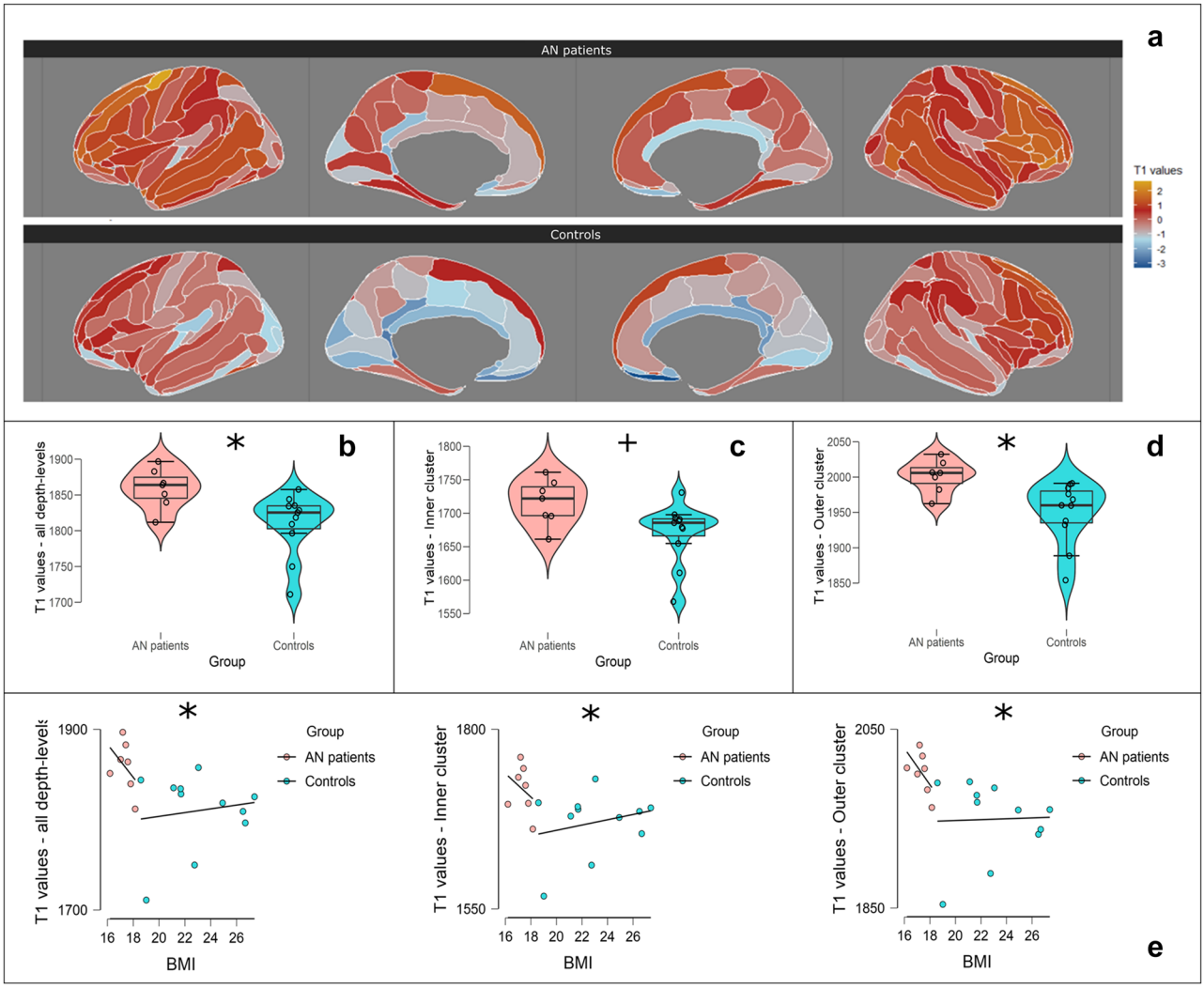

Figure 1. **(a)** Standardized total T_1 values map for AN patients (top) and controls (bottom). Maps are based on the Destrieux's Atlas and show T_1 values' average across 10 depth-levels per each Region-of-Interest (ROI) in AN patients and healthy controls. For illustrative purposes, the distribution of T1 values was rescaled to a distribution with mean = 0. **(b)** Boxplot with violin and jitter elements displaying distribution of T_1 values (in ms) as intracortical myelin concentration index averaged across all 10 cortical depth-levels for AN patients and controls; **(c)** boxplot with violin and jitter elements displaying distribution of inner cluster's T_1 values (in ms) for AN patients and controls; **(d)** boxplot with violin and jitter elements displaying distribution of outer cluster's T_1 values (in ms) for AN patients and controls; **(e)** scatterplots between BMI and T_1 values (in ms) in all depth-levels, inner and outer clusters in AN patients and controls. For illustrative purposes groups are shown separately, although the statistical significance symbol refers to the analysis on overall population. T_1 values distributions between AN patients and controls and relationship between T1 values and BMI. *$p < 0.05$; $^+p = 0.05$.

from the middle of the cortical ribbon to the gray matter/CSF boundary). The mean cortical concentration of the inner and outer clusters were included in two separate set of analyses. See Table 3 and Fig. 1c,d for details about inner and outer cluster distributions.

	AN	Controls	Group differences[a]
T_1 values (ms)—inner cluster	1716.54 (34.20)	1670.53 (45.04)	$F(1,15) = 4.32$, $p = 0.05$, $\eta^2 = 0.22$
T_1 values (ms)—outer cluster	2001.39 (23.23)	1949.38 (43.69)	$F(1,15) = 7.61$, $p = 0.01$, $\eta^2 = 0.34$

Table 3. T_1 values in the inner and outer cluster across individuals with AN and controls: Analysis of Covariance. Mean (standard deviation) of average T_1 values across cortical depth-levels 1–5 (inner cluster) and 6–10 (outer cluster). Group differences in terms of F value (degrees of freedom), p value and effect size are shown. [a]Analyses corrected for age.

Inner cluster. Patients with AN and controls had an equal variance distribution in T_1 values within the inner cluster (Levene's Test $p > 0.05$). The ANCOVA reported a difference approaching statistical significance between groups ($F(1,15) = 4.32$, $p = 0.05$, $\eta^2 = 0.22$). In the inner cluster, AN patients showed higher T_1 values in respect to controls (MD = 44.07 ms, SE = 21.20, 95% C.I. −1.11, 89.26, Cohen's d = 1.07). This result was confirmed by a bootstrapped post-hoc comparison based on 1000 replications (MD = 43.33 ms, Bias = −2.08, SE = 19.26, 95% bias corrected accelerated C.I. = 8.93, 86.58).

Outer cluster. Both groups reported equal variance distribution in T_1 values within the outer cluster (Levene's Test $p > 0.05$). The ANCOVA showed a significant effect of group on T_1 values ($F(1,15) = 7.61$, $p = 0.01$, $\eta^2 = 0.34$). In outer cluster, individuals with AN showed significantly higher T_1 values than controls (MD = 53.03 ms, SE = 19.29, 95% CI = 12.05, 95.01, Cohen's d = 1.42), confirmed by a bootstrapped post-hoc test (MD = 51.29, Bias = −1.46, SE = 15.93, 95% bias corrected accelerated C.I. = 26.66, 91.62).

Correlations between illness-related variables and intracortical myelin. At the general level BMI was negatively correlated with global T_1 values (rho = −0.68, p = 0.003, C.I. = −0.87, −0.31), T_1 values in the inner (rho = −0.57, p = 0.017, C.I. = −0.82, −0.14) and outer cluster (rho = −0.75, $p < 0.001$, C.I. = −0.90, −0.44). Visually, such correlation seems more prominent in AN patients, although within group analyses did not reveal any significant correlations ($p > 0.05$) (Fig. 1e for scatter-plots). In addition, we explored the relationship between intracortical myelin concentration, osmolality and duration of illness in AN individuals. Osmolality marginally correlated with total myelin concentration (rho = 0.79, p = 0.05, C.I. = 0.08, 0.97) and with myelin in the inner cluster (rho = 0.89, p = 0.01, C.I. 0.43, 0.98), while it was less correlated to myelin concentration in outer cluster (rho = 0.50, p = 0.27, C.I. −0.41, 0.91). Duration of illness did not correlate with total intracortical myelin concentration, inner and outer cluster myelin concentration (all $p > 0.05$).

Discussion

In this preliminary study, we used an innovative method based on 7 T ultra-high field MRI to examine depth-dependent intracortical myelin in a population of women with AN. In accordance with our hypothesis, women with AN showed higher T_1 values across the cortical ribbon. These differences were stronger in the five outermost intracortical depth-levels, whilst they were less evident in the five inner intracortical layers. Such results may index an intracortical myelin deficit in women with AN compared to healthy controls.

The use of a high-resolution MRI scanner allowed for the first time to use T_1 values as a proxy to investigate depth-dependent intracortical myelin organization in-vivo. Our results are consistent with previous findings of reduced myelin concentration in AN[27,44], and go beyond these, showing that such a deficit is widespread and mainly affects the outer depth-levels dependent intracortical myelin organization. Travis and colleagues[27] reported a relationship between decreased fractional anisotropy (FA, defined as a marker of WM integrity) and decreased relaxation time R1 (considered as an index of myelin content) in AN adolescents. This suggests that observed WM differences in AN might be due to reductions in myelination[10,45]. However, as stated recently by Barona and colleagues in their meta-analysis[46], differences in WM could be due to several factors, including a larger axon diameter, lower packing density of fibers, altered membrane permeability as well as a myelin deficit[47]. In fact, Travis and colleagues[27] also underlined that the most significant WM disruptions occurred where the axons showed the largest diameter and a thicker myelin shell (i.e. the corticospinal tract and the corpus callosum)[21].

Whereas in our study higher T_1 values were found in patients with AN, in a recent study[44] performed with a 3 T MRI scanner an opposite pattern emerged, i.e., patients with AN showed lower T_1 relaxation times (i.e. time constant indicating how long the protons need to return to the equilibrium state[41]) than controls in both gray matter and WM. Nonetheless, the authors suggested that these differences could be related to starvation-driven myelin loss[44]. Although the two interpretations seem counterintuitive, it is worth highlighting that T_1 relaxation time is strictly dependent on the physical properties of the underlying tissue[41], including free water content[48,49] and concentration and types of macromolecules[50] such as iron content[49] and myelin[51]. Thus, to date, such methodologies based on in-vivo quantitative MRI do not allow confirmation that between group differences may be due to various factors other than myelin content. Nevertheless, it is known that while water content is directly proportional to T_1 time, iron content and myelination are inversely related to T_1[41]. This is confirmed by the fact that T_1 relaxation time is generally longer in WM, which is myelin dense[41]. While Boto and colleagues[44] did not exclude the impact of water content in the measurement of relaxation times, in our study hydration level was not

a confounder. Moreover, the relationship between T_1 and myelin has also been confirmed by ex-vivo data[34,39,40,51], even in populations characterized by strong myelin loss such as multiple sclerosis[52,53].

It is known that myelin assembling persists during development and in adult life[54–57]. Animal studies highlight that the process of myelin lipid remodeling is continuous, and that the rate of change of such lipids is different throughout life[58,59]. Myelin membranes are known to have a very high lipid-to-protein ratio, with lipids accounting for at least 70% of the dry weight[2]. Myelin construction therefore requires a large amount of lipids, including cholesterol, galactolipids, plasmalogen, and fatty acids[60]. In consideration of the reduced caloric intake, decrement in intracortical myelination in AN may mirror oligodendrocytes' dysfunctions due to lack of micronutrients necessary for the synthesis of specific lipids. Nevertheless, further studies targeted on AN are needed to confirm such a claim.

A myelin deficit may also play a fundamental role in the symptomatic manifestations of AN. Animals studies suggest intracortical myelin is related to cortical functions and behavior[61], and changes in myelin preceded changes in behavior[54,55]. Therefore several authors have suggested that intracortical myelin might be a marker of plasticity in the cortex[40,61]. Myelin damage, demyelination or oligodendrocyte loss results in a global malfunction in many neurological conditions such as multiple sclerosis, leukodvstrophies, Alzheimer's disease, stroke, cerebral palsy, traumatic brain-spinal injury and cognitive decline[62,63]. Therefore intracortical myelin loss might contribute to the neurocognitive deficits of patients with AN such as cognitive flexibility, weak central coherence, emotional processing difficulties[64].

Further investigations will need to study closely the relationship between neurocognitive differences and myelin concentration in AN.

Strengths and limitations. This preliminary study is the first to investigate depth-dependent intracortical myelin organization in individuals with AN. Using the high spatial resolution afforded by 7 T imaging in conjunction with a previously validated method for intracortical myelin estimation[40] we obtained information about T_1 values used as a proxy for intracortical myelin concentration across the cortical ribbon. Given the small sample size and the lack of specific a-priori assumptions, we chose not to focus on specific ROIs and this limitation should be addressed in future studies. The small sample size represents the main limitation but the current findings albeit preliminary encourage further studies in larger and more fully characterized samples. Osmolality as an index of hydration was collected in AN patients only, precluding us from including it as a covariate in our main analysis. However, correlation between osmolality and myelin concentration in the outermost depth-levels was weaker than within the inner cluster in AN patients, and only two out of seven patients with AN had abnormal osmolality levels indicative of dehydration, hence it is unlikely that dehydration fully confounds our findings. At the time of the study, the patients were all in the acute phase of illness, but duration of illness varied across our sample. Although no relationship emerged between illness duration and variables of interest, there might have been heterogeneities in the clinical sample. Although we are aware of the aforementioned limitations, we believe that our study provides promising evidence of altered intracortical myelin organization in AN.

Conclusions

In this preliminary study, we leverage a novel method for the in-vivo examination of T_1 values as an inverse index of intracortical myelin organization in AN. We found generally higher T_1 values in women with AN compared to healthy women, mirroring a widespread lower myelin concentration. These differences might be due to malnutrition and starvation, and general brain atrophy, or might be trait markers of the illness. However, the specific mechanisms (nutritional or structural) that might lead to myelin loss, and most importantly if this loss is reversible, need to be elucidated further. Moreover given the newly hypothesized role of metabolic factors in the etiology of AN[65], whether a premorbid abnormality in myelin structure exists needs specific investigation. In a more speculative fashion, our study also raises the possibility that cognitive, visuo-spatial (and other) difficulties seen in active AN might be the result of altered intracortical myelin. Despite limitations, our findings provide an important foundation on which to build future studies. If confirmed, these results could shed new light on the neural basis of AN and on brain effects of the illness.

Methods

Participants. The study was carried out at the Icahn School of Medicine at Mount Sinai, New York. Participants were recruited amongst patients from the Mount Sinai Eating and Weight Disorders Program, the Mount Sinai Psychiatry service and from the community via flyers and adverts. Initial screen for eligibility was conducted over the phone by a research coordinator. We included female participants, with an age range from 18 to 45, who were able to provide informed consent and who spoke and understood English fluently. Patients had to have: (a) a diagnostic statistical manual of mental disorders, 5th edn (DSM-5)[66] diagnosis of AN; (b) a body mass index (BMI) between 15.5 and 18.5; (c) a history of food restriction of more than 1 year; (d) to be medically stable. Healthy controls were screened for eligibility and had to have no history of mental health disorders (including eating disorders) and no chronic medical conditions.

Exclusion criteria for all participants included any contraindication to the MRI examination (i.e., embedded or implanted metallic bodies and claustrophobia) and pregnancy.

Participants who met initial criteria for the study were invited for an in-person assessment. After providing informed consent, participants completed initial study measures and completed a urine pregnancy test. Seven female adults with current AN and 11 healthy female adults were included.

The study was approved by the institutional review committee of the Icahn School of Medicine at Mount Sinai (ISMMS). All research was performed in accordance with relevant guidelines and regulations. Patients and controls provided informed consent to participate.

Measures. Socio-demographic data were collected using a short questionnaire. Weight and height were measured objectively to calculate BMI (kg/m^2) (Table 1). Data were collected on socioeconomic status, duration of illness, and current medications in individuals with AN.

The Eating Disorder Examination interview version16.0D (EDE[67]) was used for diagnostic purposes. The EDE is a semi-structured interview considered the "gold standard" for assessing eating disorder symptoms. The EDE assesses a range of eating disorder features and yields a global score of eating disorder symptoms (Table 1).

The SCID Screening Module[68] was administered to screen participants for other psychiatric disorders conditions.

AN patients underwent a blood draw in order to establish their level of osmolality (i.e. an hydration index based on molecular weight/1 L water presence ratio expressed in milliosmoles per kilogram).

MRI acquisition. Patients and controls were scanned at the ISMMS using a 7 T MR scanner (Magnetom, Siemens Healthcare) with a 32-channel with a Nova head coil (Nova Medical, Wilmington MA). An ultra-high resolution MP2RAGE sequence was used to acquire whole brain T1-weighted images. Acquisition parameters consisted of 0.5 mm isotropic resolution, repetition time (TR) = 5000 ms, echo time (TE) = 5.75 ms, inversion time (TI) TI1/TI2 = 900 ms/2780 ms, 224 axial slices with slab thickness 11.5 cm, field-of-view $224.5 \times 203 \times 112$ mm^3, and slab selective excitation and flow suppression[36]. Bias-field corrected quantitative T1 maps and T1 images were obtained from images at the two inversion times (TI1/TI2).

High resolution intracortical myelin profiling using T_1 maps. Image preprocessing followed the procedures developed and validated previously[39,40]. Skull-stripping, background-marking and alignment (using rigid 6 degrees-of-freedom registration, normalized mutual information) to a 0.4 mm MNI template using the CBS Tools (https://www.nitrc.org/projects/cbs-tools) were applied on the T1 maps, T1-weighted and T2 images. No data were discarded due to poor quality data. Then, images were corrected for field inhomogeneities and matched to a template image[39] using 3D Slicer (https://www.slicer.org). Images were filtered with arteries and dura segmentation, corrected for partial volume effects and segmented into gray matter, white matter and cerebrospinal fluid (CSF) using the Topology-preserving, Anatomy-Driven Segmentation (TOADS)[69] and Multi-object Geometric Deformable Model (MGDM)[70] segmentation algorithms as integrated in the CBS Tools. The CRUISE algorithm[71] was applied in order to extract the cortex. Such an algorithm is robust to white matter lesions[72]. Capitalizing on the CBS Tools' Volumetric Layering module[73], the cortex was then dissected into 10 cortical depth-levels using a volume-preserving approach. This level-set approach generates one 2-dimensional surface per layer containing T_1 values at each surface location. Next, the 2-dimensional level-sets were transformed into 3-dimensional representations of T_1 values using the CBS Tools' Profile Sampling Module. This transformation represents each vertex T-values of each level-set surface as a column of identical T_1 values perpendicular to the surface[39,40]. The final result of this pipeline is 10 volumes of cortical profiles, one for each depth-level, for each of 7 patients with AN and 11 healthy controls. The whole process was completed within each individual's native space.

The cortex was then parcellated in the native space using Freesurfer (https://surfer.nmr.mgh.harvard.edu/). This parcellation was based on the pre-processed T1-weighted images alone (independent of the cortex extraction described above) and was used to obtain 148 cortical regions-of-interest (ROIs) based on the Destrieux atlas, that is particularly suitable for this type of investigation by separating gyri from sulci[73,74]. In each participant and for each cortical ROI, we estimated the absolute T_1 value as an inverse index of myelin concentration at each depth-level: so, we obtained a matrix consisting of 148 total rows (ROIs) and 10 columns (i.e. each intracortical myelin depth-level) per participant.

Statistical analyses. All demographic variables were individually checked for missing data or outliers. Normality and equality of variances were verified using Shapiro–Wilk and Levene's tests. Group comparisons for age and BMI were carried out using two-sided Independent-samples t-tests.

With the aim of getting a single index of total intra-cortical myelin concentration per participant, we averaged the values of the 10 myelin depth-measures across all the ROIs. The mean total intra-cortical myelin concentration was compared between patients and controls using an analysis of covariance (ANCOVA) with the group as main factor and age as covariate. Further, a bootstrap post-hoc comparison based on 1000 replicates was carried out in order to get a more stable group comparison result.

A Principal Component Analysis (PCA) with an oblique rotation (Promax algorithm) was applied on the original T_1 values matrix across all participants. This matrix contained of 2664 rows (148 myelin concentration values per participant, one value per ROI) and 10 columns (10 depth-levels). PCA was applied in order to reduce the number of computations and to deal with correlated predictors (i.e. T_1 values between multiple cortical depth-levels). Bartlett's Test of Sphericity has been used to check PCA assumptions. The number of components was established through a parallel analysis[75] that compared the real eigenvalues obtained from the matrix to the eigenvalues obtained from a Monte-Carlo simulated matrix based on random data with the same size[76]. As output of parallel analysis, a scree plot of eigenvalues was used to set up a threshold of significance and reliability of components using the Kaiser criterion (i.e. eigenvalues > 1). Based on the number of components extracted, we averaged the T_1 values in different analyses. Following PCA, independent comparisons between groups were carried out by means of ANCOVA with averaged T_1 values as dependent variable, the group as the main factor, age as a covariate and a bootstrap post-hoc comparison based on 1000 replicates.

Finally, for exploratory analyses, we investigated relationships between T_1 values, BMI, osmolality and duration of illness by means of non-parametric correlations (Spearman's rho rank coefficient) with significant level set at $p < 0.05$ uncorrected.

Variables	RC 1	RC 2	Uniqueness
Layer 1		0.727	0.601
Layer 2		1.042	0.054
Layer 3		0.943	0.036
Layer 4		0.804	0.035
Layer 5	0.467	0.658	0.042
Layer 6	0.627	0.500	0.043
Layer 7	0.763		0.039
Layer 8	0.903		0.033
Layer 9	1.026		0.056
Layer 10	1.038		0.145

Table 4. PCA results. Loading coefficients for RC1 and RC2 components. The first column reports all the variables included (T_1 values in cortical depth-levels from 1 to 10). RC1 and RC2 columns represent variable loadings on that specific component. Uniqueness shows the percentage of the variance of each variable not explained by the component.

All statistical analyses were carried out using JASP (https://jasp-stats.org/, v. 0.11).

Intracortical myelin clusters by principal component analysis. Bartlett's Test of Sphericity resulted significant (X^2 (26) = 19,657.73, $p < 0.001$), suggesting a redundancy in the T_1 values' matrix. Two components (RC1 and RC2) were detected by parallel analysis using an eigenvalue threshold = 1 (Kaiser criterion) (see scree plot, Fig. 1SM). Table 4 shows the contribution of each depth-measure in each component.

Specifically, T_1 values at depth levels 1 to 5 contributed to RC2, whereas those in depth levels 6–10 contributed to RC1 (a path diagram is available in Fig. 1SM). In case of participation in both components (as in the case of measures in depth levels 5 and 6), the layer was associated with the component whose expression was greater. The path diagram and scree plot available in Fig. 1SM visually confirm the contribution of each depth measure to RC1 and RC2 and the reliability of the number of components extracted from the PCA.

Data availability

The datasets generated during and/or analyzed during the current study are available from the corresponding author on reasonable request.

Received: 3 August 2021; Accepted: 5 January 2022
Published online: 16 February 2022

References

1. Alizadeh, A., Dyck, S. M. & Karimi-Abdolrezaee, S. Myelin damage and repair in pathologic CNS: Challenges and prospects. *Front. Mol. Neurosci.* **8**, 11 (2015).
2. Nave, K.-A. & Werner, H. B. Myelination of the nervous system: Mechanisms and functions. *Annu. Rev. Cell Dev. Biol.* **30**, 503–533 (2014).
3. Rowley, C. D. *et al.* Assessing intracortical myelin in the living human brain using myelinated cortical thickness. *Front. Neurosci.* **9**, 63 (2015).
4. Haroutunian, V. *et al.* Myelination, oligodendrocytes, and serious mental illness. *Glia* **62**, 1856–1877 (2014).
5. Grydeland, H., Walhovd, K. B., Tamnes, C. K., Westlye, L. T. & Fjell, A. M. Intracortical myelin links with performance variability across the human lifespan: Results from T1- and T2-weighted MRI myelin mapping and diffusion tensor imaging. *J. Neurosci. Off. J. Soc. Neurosci.* **33**, 18618–18630 (2013).
6. Bartzokis, G. *et al.* Impact on intracortical myelination trajectory of long acting injection versus oral risperidone in first-episode schizophrenia. *Schizophr. Res.* **140**, 122–128 (2012).
7. Bartzokis, G. *et al.* In vivo evidence of differential impact of typical and atypical antipsychotics on intracortical myelin in adults with schizophrenia. *Schizophr. Res.* **113**, 322–331 (2009).
8. Krigman, M. R. & Hogan, E. L. Undernutrition in the developing rat: Effect upon myelination. *Brain Res.* **107**, 239–255 (1976).
9. Wiggins, R. C. & Fuller, G. N. Relative synthesis of myelin in different brain regions of postnatally undernourished rats. *Brain Res.* **162**, 103–112 (1979).
10. Connor, J. R. & Menzies, S. L. Relationship of iron to oligodendrocytes and myelination. *Glia* **17**, 83–93 (1996).
11. Konradi, C., Sillivan, S. E. & Clay, H. B. Mitochondria, oligodendrocytes and inflammation in bipolar disorder: Evidence from transcriptome studies points to intriguing parallels with multiple sclerosis. *Neurobiol. Dis.* **45**, 37–47 (2012).
12. Andreazza, A. C., Wang, J.-F., Salmasi, F., Shao, L. & Young, L. T. Specific subcellular changes in oxidative stress in prefrontal cortex from patients with bipolar disorder. *J. Neurochem.* **127**, 552–561 (2013).
13. Patel, J. P. & Frey, B. N. Disruption in the blood-brain barrier: The missing link between brain and body inflammation in bipolar disorder?. *Neural Plast.* **2015**, 708306 (2015).
14. Arcelus, J., Mitchell, A. J., Wales, J. & Nielsen, S. Mortality rates in patients with anorexia nervosa and other eating disorders. A meta-analysis of 36 studies. *Arch. Gen. Psychiatry* **68**, 724–731 (2011).
15. Field, A. E. *et al.* Prospective association of common eating disorders and adverse outcomes. *Pediatrics* **130**, e289–e295 (2012).
16. Micali, N., Hagberg, K. W., Petersen, I. & Treasure, J. L. The incidence of eating disorders in the UK in 2000–2009: Findings from the general practice research database. *BMJ Open* **3**, 113 (2013).
17. Treasure, J. *et al.* Anorexia nervosa. *Nat. Rev. Dis. Primer* **1**, 1–21 (2015).
18. Treasure, J., Duarte, T. A. & Schmidt, U. Eating disorders. *Lancet* **395**, 899–911 (2020).

19. Frank, G. K. W., Shott, M. E. & DeGuzman, M. C. The neurobiology of eating disorders. *Child Adolesc. Psychiatr. Clin. N. Am.* **28**, 629–640 (2019).
20. Via, E. *et al.* Disruption of brain white matter microstructure in women with anorexia nervosa. *J. Psychiatry Neurosci. JPN* **39**, 367–375 (2014).
21. Nagahara, Y. *et al.* A tract-based spatial statistics study in anorexia nervosa: Abnormality in the fornix and the cerebellum. *Prog. Neuropsychopharmacol. Biol. Psychiatry* **51**, 72–77 (2014).
22. Vogel, K. *et al.* White matter microstructural changes in adolescent anorexia nervosa including an exploratory longitudinal study. *NeuroImage Clin.* **11**, 614–621 (2016).
23. Katzman, D. K., Christensen, B., Young, A. R. & Zipursky, R. B. Starving the brain: Structural abnormalities and cognitive impairment in adolescents with anorexia nervosa. *Semin. Clin. Neuropsychiatry* **6**, 146–152 (2001).
24. Kappou, K. *et al.* Neuroimaging findings in adolescents and young adults with anorexia nervosa: A systematic review. *Child. Basel Switz.* **8**, 2 (2021).
25. Phillipou, A., Rossell, S. L. & Castle, D. J. The neurobiology of anorexia nervosa: A systematic review. *Aust. N. Z. J. Psychiatry* **48**, 128–152 (2014).
26. Seitz, J., Herpertz-Dahlmann, B. & Konrad, K. Brain morphological changes in adolescent and adult patients with anorexia nervosa. *J. Neural Transm. Vienna Austria* **1996**(123), 949–959 (2016).
27. Travis, K. E. *et al.* Abnormal white matter properties in adolescent girls with anorexia nervosa. *NeuroImage Clin.* **9**, 648–659 (2015).
28. Pfuhl, G. *et al.* Preserved white matter microstructure in young patients with anorexia nervosa?. *Hum. Brain Mapp.* **37**, 4069–4083 (2016).
29. Zhang, S. *et al.* White matter abnormalities in anorexia nervosa: Psychoradiologic evidence from meta-analysis of diffusion tensor imaging studies using tract based spatial statistics. *Front. Neurosci.* **14**, 159 (2020).
30. Carey, D. *et al.* Quantitative MRI provides markers of intra-, inter-regional, and age-related differences in young adult cortical microstructure. *Neuroimage* **182**, 429–440 (2018).
31. Shafee, R., Buckner, R. L. & Fischl, B. Gray matter myelination of 1555 human brains using partial volume corrected MRI images. *Neuroimage* **105**, 473–485 (2015).
32. Whitaker, K. J. *et al.* Adolescence is associated with genomically patterned consolidation of the hubs of the human brain connectome. *Proc. Natl. Acad. Sci. U. S. A.* **113**, 9105–9110 (2016).
33. Ma, Y.-J. *et al.* Ultrashort echo time (UTE) magnetic resonance imaging of myelin: Technical developments and challenges. *Quant. Imaging Med. Surg.* **10**, 1186–1203 (2020).
34. Fracasso, A. *et al.* Lines of Baillarger in vivo and ex vivo: Myelin contrast across lamina at 7T MRI and histology. *Neuroimage* **133**, 163–175 (2016).
35. Waehnert, M. D. *et al.* A subject-specific framework for in vivo myeloarchitectonic analysis using high resolution quantitative MRI. *Neuroimage* **125**, 94–107 (2016).
36. Marques, J. P. *et al.* MP2RAGE, a self bias-field corrected sequence for improved segmentation and T1-mapping at high field. *Neuroimage* **49**, 1271–1281 (2010).
37. Sanchez-Panchuelo, R. M., Francis, S., Bowtell, R. & Schluppeck, D. Mapping human somatosensory cortex in individual subjects with 7T functional MRI. *J. Neurophysiol.* **103**, 2544–2556 (2010).
38. Tardif, C. L. *et al.* Multi-contrast multi-scale surface registration for improved alignment of cortical areas. *Neuroimage* **111**, 107–122 (2015).
39. Dinse, J. *et al.* A cytoarchitecture-driven myelin model reveals area-specific signatures in human primary and secondary areas using ultra-high resolution in-vivo brain MRI. *Neuroimage* **114**, 71–87 (2015).
40. Sprooten, E. *et al.* Depth-dependent intracortical myelin organization in the living human brain determined by in vivo ultra-high field magnetic resonance imaging. *Neuroimage* **185**, 27–34 (2019).
41. Deichmann, R. & Gracien, R.-M. T1: Longitudinal relaxation time 1. in *Quantitative MRI of the Brain: Principles of Physical Measurement* (CRC Press, 2018).
42. Schnure, J. J. & Leahy, J. L. Chapter 50—Diabetic ketoacidosis and hyperosmolar hyperglycemic state. in *Critical Care Secrets*. 5th edn. 359–368. (eds. Parsons, P. E. & Wiener-Kronish, J. P.). https://doi.org/10.1016/B978-0-323-08500-7.00065-5 (Mosby, 2013).
43. Mowinckel, A. M. & Vidal-Piñeiro, D. Visualization of brain statistics with R packages ggseg and ggseg3d. *Adv. Methods Pract. Psychol. Sci.* **3**, 466–483 (2020).
44. Boto, J. *et al.* Cerebral gray and white matter involvement in anorexia nervosa evaluated by T1, T2, and T2* mapping. *J. Neuroimaging* **29**, 598–604 (2019).
45. Stüber, C. *et al.* Myelin and iron concentration in the human brain: A quantitative study of MRI contrast. *Neuroimage* **93**(Pt 1), 95–106 (2014).
46. Barona, M. *et al.* White matter alterations in anorexia nervosa: Evidence from a voxel-based meta-analysis. *Neurosci. Biobehav. Rev.* **100**, 285–295 (2019).
47. Jones, D. K., Knösche, T. R. & Turner, R. White matter integrity, fiber count, and other fallacies: The do's and don'ts of diffusion MRI. *Neuroimage* **73**, 239–254 (2013).
48. Fatouros, P. P., Marmarou, A., Kraft, K. A., Inao, S. & Schwarz, F. P. In vivo brain water determination by T1 measurements: Effect of total water content, hydration fraction, and field strength. *Magn. Reson. Med.* **17**, 402–413 (1991).
49. Gelman, N., Ewing, J. R., Gorell, J. M., Spickler, E. M. & Solomon, E. G. Interregional variation of longitudinal relaxation rates in human brain at 3.0 T: Relation to estimated iron and water contents. *Magn. Reson. Med.* **45**, 71–79 (2001).
50. Rooney, W. D. *et al.* Magnetic field and tissue dependencies of human brain longitudinal 1H2O relaxation in vivo. *Magn. Reson. Med.* **57**, 308–318 (2007).
51. Lutti, A., Dick, F., Sereno, M. I. & Weiskopf, N. Using high-resolution quantitative mapping of R1 as an index of cortical myelination. *Neuroimage* **93**, 176–188 (2014).
52. Mottershead, J. P. *et al.* High field MRI correlates of myelin content and axonal density in multiple sclerosis—A post-mortem study of the spinal cord. *J. Neurol.* **250**, 1293–1301 (2003).
53. Schmierer, K. *et al.* Quantitative magnetic resonance of postmortem multiple sclerosis brain before and after fixation. *Magn. Reson. Med.* **59**, 268–277 (2008).
54. Liu, J. *et al.* Impaired adult myelination in the prefrontal cortex of socially isolated mice. *Nat. Neurosci.* **15**, 1621–1623 (2012).
55. Makinodan, M., Rosen, K. M., Ito, S. & Corfas, G. A critical period for social experience-dependent oligodendrocyte maturation and myelination. *Science* **337**, 1357–1360 (2012).
56. Mangin, J.-M., Li, P., Scafidi, J. & Gallo, V. Experience-dependent regulation of NG2 progenitors in the developing barrel cortex. *Nat. Neurosci.* **15**, 1192–1194 (2012).
57. Snaidero, N. & Simons, M. Myelination at a glance. *J. Cell Sci.* **127**, 2999–3004 (2014).
58. Ando, S., Tanaka, Y., Toyoda, Y. & Kon, K. Turnover of myelin lipids in aging brain. *Neurochem. Res.* **28**, 5–13 (2003).
59. Poitelon, Y., Kopec, A. M. & Belin, S. Myelin fat facts: An overview of lipids and fatty acid metabolism. *Cells* **9**, 812 (2020).
60. Yoon, H. *et al.* Interplay between exercise and dietary fat modulates myelinogenesis in the central nervous system. *Biochim. Biophys. Acta BBA Mol. Basis Dis.* **1862**, 545–555 (2016).
61. Micheva, K. D. *et al.* A large fraction of neocortical myelin ensheathes axons of local inhibitory neurons. *Elife* **5**, 1–29 (2016).
62. Fields, R. D. Myelin—More than insulation. *Science* **344**, 264–266 (2014).

63. Langley, M. R., Triplet, E. M. & Scarisbrick, I. A. Dietary influence on central nervous system myelin production, injury, and regeneration. *Biochim. Biophys. Acta BBA Mol. Basis Dis.* **1866**, 165779 (2020).
64. Kanakam, N. & Treasure, J. A review of cognitive neuropsychiatry in the taxonomy of eating disorders: State, trait, or genetic?. *Cognit. Neuropsychiatry* **18**, 83–114 (2013).
65. Watson, H. J. *et al.* Genome-wide association study identifies eight risk loci and implicates metabo-psychiatric origins for anorexia nervosa. *Nat. Genet.* **51**, 1207–1214 (2019).
66. APA. *Diagnostic and Statistical Manual of Mental Disorders.* 5th edn. (APA, 2013).
67. Fairburn, C. G., Cooper, Z. & O'connor, M. E. Eating disorder examination (edition 16.0 D). *Cogn. Behav. Ther. Eat. Disord.* **309**, 265–308 (2008).
68. First, M. B., Spitzer, R. L., Gibbon, M. & Williams, J. B. *Structured Clinical Interview for DSM-IV-TR Axis I Disorders, Research Version, Patient Edition*. (2002).
69. Bazin, P.-L. & Pham, D. L. Topology-preserving tissue classification of magnetic resonance brain images. *IEEE Trans. Med. Imaging* **26**, 487–496 (2007).
70. Bazin, P.-L. *et al.* A computational framework for ultra-high resolution cortical segmentation at 7 Tesla. *Neuroimage* **93**(Pt 2), 201–209 (2014).
71. Landman, B. A. *et al.* System for integrated neuroimaging analysis and processing of structure. *Neuroinformatics* **11**, 91–103 (2013).
72. Shiee, N. *et al.* Reconstruction of the human cerebral cortex robust to white matter lesions: Method and validation. *Hum. Brain Mapp.* **35**, 3385–3401 (2014).
73. Waehnert, M. D. *et al.* Anatomically motivated modeling of cortical laminae. *Neuroimage* **93**(Pt 2), 210–220 (2014).
74. Sereno, M. I., Lutti, A., Weiskopf, N. & Dick, F. Mapping the human cortical surface by combining quantitative T(1) with retinotopy. *Cereb. Cortex N. Y. N* **1991**(23), 2261–2268 (2013).
75. Horn, J. L. A rationale and test for the number of factors in factor analysis. *Psychometrika* **30**, 179–185 (1965).
76. Allen, M. *The SAGE Encyclopedia of Communication Research Methods*. (SAGE Publications, 2017).

Acknowledgements

This work was supported by a Brain and Behavior Research Foundation Independent Investigator award to NM.

Author contributions

E.P. and G.E.D. analyzed the data and wrote the main manuscript text. B.B. and S.F. wrote the main manuscript text. A.H. collected the data. N.M. designed the study, led data collection, data analysis, and writing of the main manuscript. All authors reviewed the manuscript.

Competing interests

The authors declare no competing interests.

Additional information

Supplementary Information The online version contains supplementary material available at https://doi.org/10.1038/s41598-022-06113-x.

Correspondence and requests for materials should be addressed to N.M.

Reprints and permissions information is available at www.nature.com/reprints.

Publisher's note Springer Nature remains neutral with regard to jurisdictional claims in published maps and institutional affiliations.